

# Push–Pull Acyl-Phosphine Oxides for Two-Photon-Induced Polymerization

Rashid Nazir,<sup>†</sup> Paulius Danilevicius,<sup>‡</sup> David Gray,<sup>‡</sup> Maria Farsari,<sup>‡,\*</sup> and Daniel T. Gryko<sup>†,§,\*</sup>

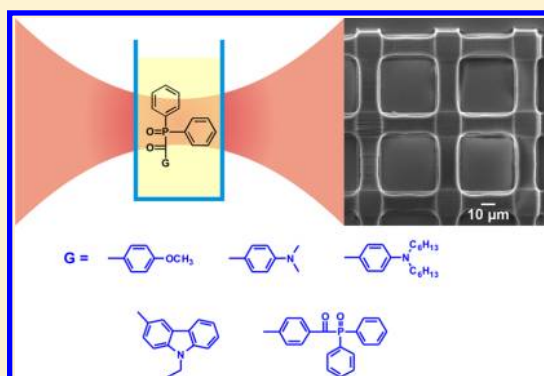
<sup>†</sup>Faculty of Chemistry, Warsaw University of Technology, Noakowskiego 3, 00-664 Warsaw, Poland

<sup>‡</sup>Institute of Electronic Structure and Laser (IESL), Foundation for Research and Technology Hellas (FORTH), P.O. Box 1527, 711 10 Heraklion, Crete, Greece

<sup>§</sup>Institute of Organic Chemistry, Polish Academy of Sciences, Kasprzaka 44/52, Warsaw, Poland

## Supporting Information

**ABSTRACT:** The two-step method for the synthesis of acyl–phosphine oxides from aromatic aldehydes was optimized giving the products in 52–97% overall yield. Linear and nonlinear optical properties of series of acyl–phosphine oxides possessing substituents with different electron-donating ability were investigated. Two-photon absorption cross sections ( $\sigma_2$ ) of push–pull acyl–phosphine oxide was determined as 9GM via z-scan measurements with femtosecond laser pulses. Using acyl–phosphine oxides possessing dipolar structure as initiators, 3D nanopatterns were successfully fabricated by two-photon initiated polymerization. These compounds also initiate classical photopolymerization when excited with UV radiation.



## INTRODUCTION

Two-photon-induced photopolymerization (TPIP) has been intensively studied recently as the interest in the direct laser writing of high-resolution three-dimensional (3D) structures has increased.<sup>1</sup> The technique is based on the two-photon polymerization (2PP) of photosensitive materials; when the beam of an ultrafast laser is tightly focused within the volume of such a transparent material, the polymerization process can be initiated by nonlinear absorption within the focal volume. By moving the beam focus through the resin in three dimensions, 3D structures can be fabricated. TPIP is a solid free-form fabrication technique where a resin, usually containing a variety of acrylate, epoxy, or hybrid materials and a photoinitiator (PI), is cured inside the focal voxel of the laser. To obtain an efficient and clean polymerization and therefore high-quality structures, highly active two-photon absorption (TPA) PI plays a key role. The method has been exploited in various applications, such as photonic crystals,<sup>2</sup> mechanical devices<sup>3,4</sup> and biomolecule scaffolds.<sup>5</sup> Resolution as high as 9 nm has been reported recently.<sup>6</sup>

TPIP provides excellent spatial control due to the confinement of the photoactivated polymerization within the focal volume of the laser beam.<sup>7</sup> Moreover, as the material is transparent to the excitation wavelength (usually 530–800 nm), it is possible to penetrate into the volume of the resin<sup>8</sup> and there is reduced scattering. In addition, as the laser pulse length is in the picosecond or femtosecond range, there are reduced additional thermal or photochemical side reactions. A competent TPIP process requires active two-photon absorption

photoinitiators (TPA PIs), which ensure high writing speeds and a low polymerization threshold.

To date, there has been limited research into PIs specially designed for TPIP. PIs designed for one-photon lithography are commonly used.<sup>9</sup> However, as these PIs have rather low TPA cross sections ( $\sigma_2$ )<sup>10</sup> high excitation power and long exposure time are required, which often result in damage to the polymeric structures. The development of practical two-photon absorption photoinitiators (TPA PIs) has been slow due to their complex syntheses often utilizing expensive catalysts. These shortcomings have been a critical barrier for further advances in the promising field of two-photon-induced photopolymerization (TPIP) technology. Recently several groups reported good results for  $\alpha,\beta$ -unsaturated ketones as TPA PIs.<sup>10b,c</sup>

We aimed to study the possibilities to overcome this disadvantage, by designing and synthesizing a new generation of photoinitiators possessing at the same time large  $\sigma_2$  and high yield of radical photoinitiating. While designing new photoinitiators we followed well-known principles proving that dipolar (D– $\pi$ –A) chromophores typically possess larger  $\sigma_2$  than compounds with uniform electron distribution.<sup>11</sup> Herein we would like to present the new generation of acyl–phosphine oxide photoinitiators designed toward favorable combination of

Received: May 25, 2013

Revised: September 2, 2013

large two-photon absorption cross section and high yield radical photoinitiating.

## EXPERIMENTAL SECTION

**Synthesis.** All commercially available compounds were used as received. All solvents were dried and distilled prior to use. Transformation and oxygen sensitive compounds were performed under argon atmosphere. The reaction progress was monitored by means of thin layer chromatography (TLC) which was performed on aluminum sheets, coated with silica gel 60 F254 (Merck) or aluminum oxide 60 F254 (neutral Merck) with detection by a UV lamp. Product purification was done by means of column chromatography with silica flash P 60 (40–63  $\mu$ m, SiliCycle) or aluminum oxide 90 (neutral, 70–230 mesh, Merck), dry column vacuum chromatography (DCVC) with silica (MN-Kieselgel P/UV254) or Aluminum oxide (MN-Aluminumoxid G). Identity and purity of prepared compounds were proved by  $^1\text{H}$  NMR and  $^{13}\text{C}$  NMR (Varian 500/200 MHz). High-resolution mass spectra (ESI HRMS) were obtained on MaldiSY-NAPT G2-S HDMS/GCT Premier, Waters. The following compounds: diphenylphosphine oxide (DPO),<sup>12</sup> **1c**<sup>13</sup> and **1d**<sup>14</sup> were obtained as described in literature.

**General Procedure for the Preparation of  $\alpha$ -Hydroxybenzylphosphine Oxides (2a–2d).** To solution of aromatic aldehyde (1.0 mmol) and diphenylphosphine oxide (202 mg, 1.0 mmol) in tetrahydrofuran (10 mL), triethylamine (0.15 mL, 1.0 mmol) was added dropwise. The reaction was stirred at room temperature for 4 h (TLC analysis). The solvent was concentrated under vacuum and the crude product was purified by recrystallization or by column chromatography.

**$\alpha$ -Hydroxy(4-methoxybenzyl)diphenylphosphine Oxide (2a).** The crude product was purified by recrystallization from toluene as a white crystals in 98% yield. Physical properties concur with the published data.<sup>15</sup>

**$\alpha$ -Hydroxy(4-dimethylaminobenzyl)diphenylphosphine Oxide (2b).** The crude product was purified by recrystallization from toluene as yellow crystals in 94% yield.  $^1\text{H}$  NMR (500 MHz,  $\text{CDCl}_3$ ):  $\delta$  7.33–7.80 (m, 10H), 7.015 (dd  $J_1 = 1.5$  Hz,  $J_2 = 2$  Hz, 2H), 6.53 (d,  $J = 8.5$  Hz), 5.343 (d,  $J = 4$  Hz), 4.14 (s, 1H), 2.88 (s, 1H).  $^{13}\text{C}$  NMR (500 MHz,  $\text{CDCl}_3$ ):  $\delta$  150.5, 132.5, 132.4, 132.1, 132.0, 131.8, 131.3, 130.5, 129.6, 128.8, 128.7, 128.4, 128.3, 128.3, 128.2, 112.5, 74.3 (d,  $J = 334.5$  Hz), 40.8. HRMS (ESI):  $m/z$  ( $[\text{M} + \text{Na}]^+$ ) calcd for  $\text{C}_{21}\text{H}_{22}\text{NO}_2\text{PNa}$ , 374.1286; found, 374.1286.

**$\alpha$ -Hydroxy(4-diethylaminobenzyl)diphenylphosphine Oxide (2c).** Purification by column chromatography (Hex:EtOAc = 5:1) yielded the product as yellow crystals with a yield of 91%.  $^1\text{H}$  NMR (500 MHz,  $\text{CDCl}_3$ ):  $\delta$  7.84–7.34 (m, 10H), 6.98 (d,  $J = 7.5$  Hz, 2H), 6.45 (d,  $J = 9$  Hz, 2H), 5.33 (s, 1H), 3.20 (t,  $J = 15.5$  Hz, 4H), 1.52–1.51 (m, 4H), 1.31–1.29 (m, 4H), 0.89 (t,  $J = 13.5$  Hz, 6H).  $^{13}\text{C}$  NMR (500 MHz,  $\text{CDCl}_3$ ):  $\delta$  147.2, 133.8, 132.1, 131.8, 131.7, 131.5, 131.4, 131.4, 131.2, 131.1, 131.0, 130.9, 128.9, 128.9, 128.4, 128.3, 128.1, 128.1, 128.0, 127.9, 123.7, 110.4, 72.3 (d,  $J = 354$  Hz), 50.7, 31.1, 26.7, 26.0, 22.1, 13.8. HRMS (ESI):  $m/z$  ( $[\text{M} + \text{H}]^+$ ) calcd for  $\text{C}_{31}\text{H}_{43}\text{NO}_2\text{P}$ , 492.3031; found, 492.3033.

**(9-Ethylcarbazol-3-yl)(hydroxymethyl)diphenylphosphine Oxide (2d).** The solid was filtered and washed with THF and purified by recrystallization from toluene as light yellow crystals in 88% yield.  $^1\text{H}$  NMR (500 MHz,  $\text{CDCl}_3$ ):  $\delta$  7.99 (s, 1H), 7.95 (d,  $J = 8$  Hz, 1H), 7.88 (q,  $J = 27.5$  Hz), 7.57–7.41 (m, 9H), 7.34 (d,  $J = 8$  Hz, 1H), 7.18 (d,  $J = 15$  Hz, 1H), 6.51 (dd  $J_1 = 5.5$  Hz,  $J_2 = 6$  Hz, 1H), 5.78 (t,  $J = 11.5$  Hz, 1H), 4.40 (q,  $J = 21$  Hz, 2H), 1.28 (t,  $J = 14$  Hz, 3H).  $^{13}\text{C}$  NMR (500 MHz,  $\text{CDCl}_3$ ):  $\delta$  132.2, 132.2, 132.1, 132.0, 128.7, 128.3, 126.8, 124.9, 121.2, 120.6, 109.2, 108.6, 37.9, 13.9. HRMS (ESI):  $m/z$  ( $[\text{M} + \text{Na}]^+$ ) calcd for  $\text{C}_{27}\text{H}_{24}\text{NO}_2\text{PNa}$ , 448.1442; found, 448.1443.

**1,4-Phenylenebis(diphenylphosphoryl)methanol (2e).** To solution of terephthalaldehyde (134 mg, 1.0 mmol) and diphenylphosphine oxide (404 mg, 2.0 mmol) in tetrahydrofuran (15 mL) was added dropwise triethylamine (0.30 mL, 2.0 mmol). The reaction was stirred at room temperature for 24 h (TLC analysis). The reaction mixture was stirred for 24 h, and during this period, the product precipitated. The solid was filtered and washed with THF, dried, and

used without further purification for next step. Yield of crude product was 81%.

**General Procedure for the Synthesis of Benzoyldiphenylphosphine Oxides (3a–3d).** A solution of  $\alpha$ -hydroxybenzylphosphine oxides (0.5 mmol) and  $\text{MnO}_2$  (870 mg, 10 mmol) in dichloromethane (10 mL) was stirred at room temperature for 18 h until the complete of reaction (TLC analysis). The reaction mixture was filtered through Celite, solvent was concentrated under vacuum, and the crude product was purified by recrystallization or by column chromatography.

**4-Methoxybenzoyldiphenylphosphine Oxide (MBDPO) (3a).** The crude product was purified by recrystallization from cyclohexane as white crystals in 99% yield. Its physical properties concur with the published data.<sup>16</sup>

**4-Dimethylaminobenzoyldiphenylphosphine Oxide (DMABDPO) (3b).** The crude product was purified by recrystallization from toluene as yellow crystals in 93% yield.  $^1\text{H}$  NMR (500 MHz,  $\text{CDCl}_3$ ):  $\delta$  8.50 (d,  $J = 9$  Hz, 2H), 7.90–7.86 (m, 4H), 7.51–7.44 (m, 6H), 6.64 (d,  $J = 9$  Hz), 3.063 (s, 1H).  $^{13}\text{C}$  NMR (500 MHz,  $\text{CDCl}_3$ ):  $\delta$  199.2 (carbonyl, d, 327 Hz), 154.6, 133.0, 132.08, 132.06, 132.04, 131.9, 131.6, 130.9, 129.0, 128.5, 128.4, 126.4, 126.0, 110.9, 40.0. HRMS (ESI):  $m/z$  ( $[\text{M} + \text{Na}]^+$ ) calcd for  $\text{C}_{21}\text{H}_{20}\text{NO}_2\text{PNa}$ , 372.1129; found, 372.1125.

**4-Diethylaminobenzoyldiphenylphosphine Oxide (DHABDPO) (3c).** Purification by column chromatography (Hex:EtOAc = 5:1) yielded the product of as yellow oil in 97% yield.  $^1\text{H}$  NMR (500 MHz,  $\text{CDCl}_3$ ):  $\delta$  8.46 (d,  $J = 9.0$  Hz, 2H), 7.91–7.87 (m, 4H), 7.53–7.43 (m, 6H), 6.58 (d,  $J = 9.0$  Hz, 2H), 3.32 (t,  $J = 15.5$  Hz, 4H), 1.59–1.57 (m, 4H), 1.30–1.25 (m, 4H), 0.89 (t,  $J = 13.5$  Hz, 6H).  $^{13}\text{C}$  NMR (500 MHz,  $\text{CDCl}_3$ ):  $\delta$  198.0 (carbonyl, d, 329 Hz), 153.0, 133.2, 132.7, 132.0, 132.0, 131.9, 131.8, 131.0, 130.8, 130.7, 129.0, 128.9, 128.5, 128.4, 125.4, 110.7, 51.2, 31.7, 27.2, 26.7, 22.7, 14.1. HRMS (ESI):  $m/z$  ( $[\text{M} + \text{Na}]^+$ ) calcd for  $\text{C}_{31}\text{H}_{40}\text{NO}_2\text{PNa}$ , 512.27; found, 512.2708.

**9-Ethylcarbazolebenzoyldiphenylphosphine Oxide (CBDPO) (3d).** The crude product was purified by recrystallization from toluene as a yellow crystal with a yield 91%.  $^1\text{H}$  NMR (500 MHz,  $\text{CDCl}_3$ ):  $\delta$  9.50 (d,  $J = 1.5$  Hz, 1H), 8.70 (dd  $J_1 = 1.5$  Hz,  $J_2 = 1.5$  Hz, 1H), 8.20 (d,  $J = 8$  Hz, 1H), 7.97–7.93 (m, 4H), 7.55–7.41 (m, 10H), 4.39 (q,  $J = 22$  Hz, 2H), 1.45 (t,  $J = 14$  Hz, 3H).  $^{13}\text{C}$  NMR (500 MHz,  $\text{CDCl}_3$ ):  $\delta$  202.3 (carbonyl, d, 323 Hz), 143.8, 140.7, 132.29, 132.28, 132.1, 132.0, 131.3, 130.6, 129.6, 129.2, 128.7, 128.6, 128.3, 126.8, 124.9, 123.5, 123.2, 121.2, 120.6, 109.2, 108.6, 37.9, 13.9. HRMS (ESI):  $m/z$  ( $[\text{M} + \text{Na}]^+$ ) calcd for  $\text{C}_{27}\text{H}_{22}\text{NO}_2\text{PNa}$ , 446.1286; found, 446.1287.

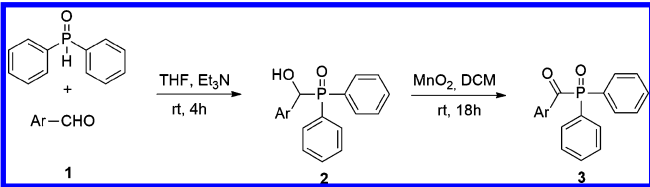
**Phthanoyl Bis(diphenylphosphine oxide) (PBDPO) (3e).** A solution of **2e** (538 mg, 1.0 mmol) and manganese dioxide ( $\text{MnO}_2$ ) (1.74 g, 20 mmol) in 10 mL of dichloromethane ( $\text{CH}_2\text{Cl}_2$ ) was stirred for 18 h until the complete of reaction (TLC analysis). The reaction mixture filter through Celite, solvent was concentrated under vacuum and the crude product was purified by recrystallization with toluene with yield 64%. Physical properties concur with the published data.<sup>17a</sup>

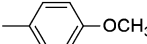
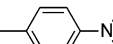
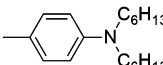
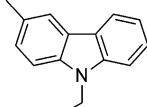
**4,4-Bis(diethylamino)benzophenone (R).** 4,4-Bis(diethylamino)benzophenone (R), otherwise known as Michler's ketone, was used for reference, as it is used as a two-photon initiator by many research groups.<sup>17b</sup> It was obtained from Aldrich and used without further purification.

**z-Scan Technique.** In order to investigate the TPA sensitivity of our compounds, we used the z-scan technique to measure the TPA cross-section. The z-scan technique is based on the change of the material's properties while traversing the focus of a laser beam. To measure the TPA cross-section, the change in the material's transmission was monitored. When approaching the waist of the beam, the intensity is high enough to induce nonlinearity. If the sample exhibits TPA, a decrease in light transmittance can be observed, depending on the sample position with respect to the beam waist. Fitting the transmittance versus the sample position to the following equation allows the TPA cross-section to be extracted.<sup>18</sup>

$$T(z) = \sum_{n=0}^{\infty} \frac{(-q_0)^n}{(n+1)^{3/2}(1+x^2)^n} \quad (1)$$

Table 1. Results of Two-Step Synthesis of Acyl-Phosphine Oxides 3a–3d



Ar	Aldehyde	Alcohol	Yield	Acyl-phosphine oxide	Yield
	<b>1a</b>	<b>2a</b>	98%	<b>3a</b>	99%
	<b>1b</b>	<b>2b</b>	94%	<b>3b</b>	93%
	<b>1c</b>	<b>2c</b>	91%	<b>3c</b>	97%
	<b>1d</b>	<b>2d</b>	88%	<b>3d</b>	91%

where  $q_0 = I_0 L_{\text{eff}} N_A \rho \times 10^{-3} \sigma_0 \lambda / hc$ ,  $I_0$  is the laser intensity in the waist of the beam, which is calculated as  $I_0 = 2E / \pi^{3/2} \tau w_0^2$ ,  $E$  is the laser pulse energy,  $\tau$  is the pulse duration,  $w_0$  is the beam waist radius,  $L_{\text{eff}}$  is the effective sample thickness, which is expressed as  $L_{\text{eff}} = (1 - e^{-\alpha L}) / \alpha$ ,  $\alpha$  is the single-photon absorption coefficient,  $L$  is the sample thickness (1 mm thick cuvette was used in our experiment),  $N_A$  is the Avogadro constant,  $\rho$  is the concentration of the sample in mol/L,  $\lambda$  is the wavelength of the laser,  $h$  is the Planck constant,  $c$  is the speed of light,  $\sigma_2$  is two-photon absorption cross-section,  $x = z/z_0$ ,  $z$  is sample position, and  $z_0$  is Rayleigh length

The laser source used is a regenerative Ti:sapphire amplifier, operating at 800 nm, with 250 fs pulses and a repetition rate of 1 kHz. The laser beam was focused with a lens of 10 mm focal length into a solution of our compounds in a 1 mm path-length cuvette. The sample was translated with a motorized stage along the beam propagation axis and the light transmittance was measured with a photodiode (DET100A, Thorlabs). The same type of photodiode was used as a reference where part of the incident beam was sampled before the sample in order to correct for fluctuations in the laser. The sample movement, correction of laser energy fluctuations and data collection was automated with custom-made Lab VIEW software.

**TPIP Setup.** The TPIP setup used for the fabrication 3D structures has been described previously.<sup>19</sup> In this work, the light source used was a Ti:sapphire femtosecond laser operating at 800 nm with a repetition rate of 75 MHz (Femtolasers Fusion). This source is a compact diode-pumped femtosecond laser oscillator with integrated dispersive mirrors that precompensate the beam delivery and focusing optics to achieve sub-20 fs duration pulses into the sample. The laser beam was tightly focused into the volume of the photosensitive hybrid material using a high numerical aperture microscope objective lens (100X, N.A. = 1.4, Zeiss, Plan Apochromat). Sample movement in *xyz* was achieved using piezoelectric stages (Physikal Instrumente). The TPIP procedure was controlled through a computer using the 3DPoli software. The average laser power needed for the fabrication of 3D structures was 20–40 mW, measured before the objective (average transmission 20%), and the scanning velocity was 20  $\mu\text{m/s}$ .

The material used for the fabrication of 3D structures is a composite hybrid material based on zirconium and silicon oxides. Its synthesis has been described elsewhere.<sup>20</sup>

## RESULTS AND DISCUSSION

Both acyl-phosphine oxides and acyl-phosphonates are known to be used as classical (i.e., one-photon) photoinitiators, for example, to produce model polymers for dental applications.<sup>21</sup> From the point of targeted dipolar structure these classes of compounds possess one obvious advantage—the functionality, which is responsible for photoinitiating activity is at the same time very strong electron-withdrawing group. In consequence, by adding suitable donor functionality, one can create push–pull systems.

Two methods are known for the synthesis of  $\alpha$ -carbonylphosphine oxides. The classical one, consisting of reaction of acid chlorides with alkoxyphosphine oxide, is straightforward but suffers from limited availability of acid chlorides.<sup>22</sup> The alternative, two-step methodology has been developed by Su and co-workers. Initial addition of aldehydes to diphenylphosphine oxide in toluene in the presence of sodium methanolate as catalyst, gives  $\alpha$ -hydroxyphosphine oxides, which are oxidized to desired acyl-phosphine oxides by vanadyl acetylacetonate or  $\text{MnO}_2$ .<sup>23,24</sup>

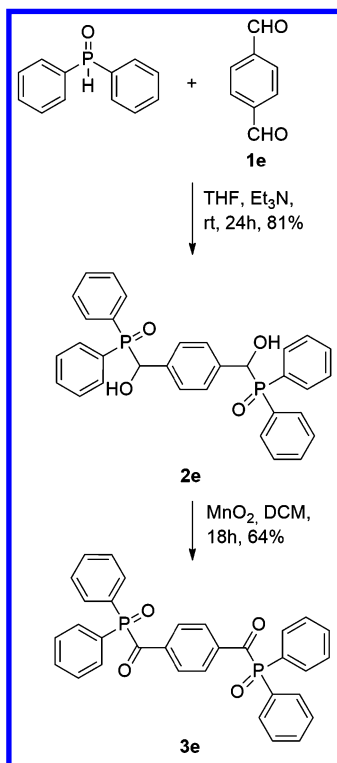
We decided to explore the second methodology since its scope is potentially broader and it allows to start from various, commercially available aromatic aldehydes. The addition of 4-methoxybenzaldehyde to diphenylphosphine oxide has been chosen as model reaction (Table 1). The first step was performed by following the protocol reported by Wan et al.<sup>25</sup> Thus, reaction of aldehyde **1a** with  $\text{Ph}_2\text{HPO}$  catalyzed by triethylamine gave  $\alpha$ -hydroxyphosphine oxide **2a** in 98% yield (Table 1). The oxidation step proved more difficult. Variety of oxidants such as chromium trioxide, potassium permanganate, iodobenzenediacetate, vanadyl acetylacetonate, manganese dioxide, and pyridinium dichromate were tested. Among them only  $\text{MnO}_2$  in DCM gave satisfactory yield without decomposition of starting material **2a**. Subsequently we applied these optimized protocol to synthesize the other acyl-phosphine oxides (Table 1). Moderately electron-rich MeO group has been replaced with stronger donor ( $\text{Me}_2\text{N}$ ) (Table



1). Its better soluble analogue **3c** has been also synthesized along with carbazole derivative **3d** (Table 1).

Having such efficient methodology in hand we wondered if it would be able to lead to compounds possessing two acylphosphine oxides moieties. The double addition of terephthalaldehyde followed by oxidation led to bis-oxide **3e** (possessing an A- $\pi$ -A type of structure) in 52% overall yield (Scheme 1).

Scheme 1



Subsequently, linear optical properties of compounds **3a–3e** have been then examined (Figure 1). Compounds **3a** and **3e** absorb only UV-radiation, while distinctly yellow dyes **3b–d** have  $\lambda_{\text{max}} \sim 390$  nm (Figure 1). This absorption of violet light allowed us to draw conclusion that their two-photon absorption

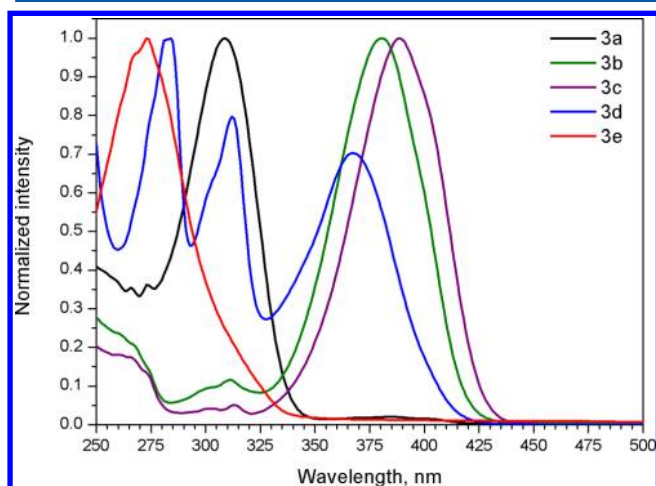


Figure 1. Absorption spectra of compounds **3a** (black line), **3b** (green line), **3c** (purple line), **3d** (blue line), and **3e** (red line) in chloroform.

will be located around 800 nm, which should enable to use a Ti:sapphire femtosecond laser for nonlinear experiments.

Two-photon absorption was studied via *z*-scan measurements. Figure 2 shows the normalized laser intensity trans-

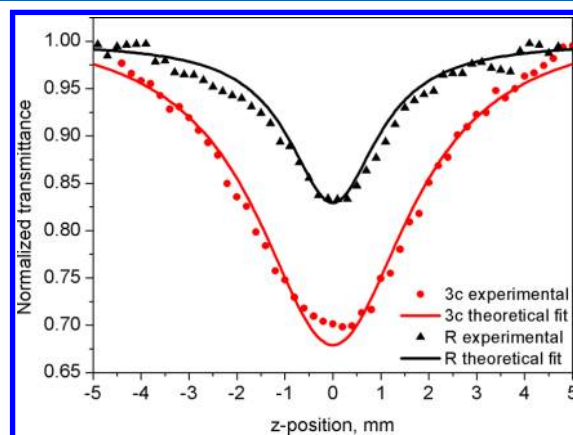


Figure 2. *z*-Scan data from measurements of the compound **3c** [0.15 M solution in methanol, 223 GW/cm<sup>2</sup> laser intensity], and compound **R** [0.25 M solution in methanol, 115 GW/cm<sup>2</sup> laser intensity]. Dots correspond to experimental data points and the curves are the best fit from eq 1.

mittance dependence on the sample position. The reduction of the transmittance around the focal spot of the laser beam indicates TPA in the compounds **3c** and **R**. By fitting this data with eq 1, we retrieved the TPA cross-section of the compounds **3c** and **R**, which are the 9GM and 6GM respectively. Similar value has been obtained for compound **3b**, but cross sections of all other compounds were lower than this value, but not accurately measurable as they are below the signal-to-noise ratio for this experiment.

The one-photon capability of the synthesized photoinitiators was confirmed by polymerizing drop-cast films of the material using a wide-spectrum UV lamp.

Finally, TPIP structuring tests at different laser intensities and feed rates were performed to evaluate the TPA initiation efficiency of each initiator. Ideal building parameters for each initiator were determined by changing the laser intensity, the feed rate, and the shape size using the same molar PI concentrations. For the 3D-structure fabrication, we chose the woodpile photonic crystal geometry.<sup>26</sup> This is widely used and well characterized and allows us to compare the material structurability and resolution with our previous results, and those of other groups using TPIP.<sup>2b,27</sup> It was possible to fabricate good quality 3D Woodpile structures using the compounds **2b**, **3b**, **3c**, and **3d**. Figure 3 shows such an example of 3D-structure fabricated using the zirconium–silicon hybrid described in<sup>20</sup> and 1% wt of the compound **3c** as a radical initiator. The distance between consecutive lines is 500 nm. The highest lateral resolution achieved was in the order of 300 nm.

It should be pointed out that while two different laser systems were used for the photopolymerization and the *z*-scan measurements (a Ti:sapphire oscillator and a regenerative Ti:sapphire amplifier, respectively), when the experimental conditions are taken into account, it can be calculated that the photon flux density is the similar in both cases and in the order of  $10^{29}$  photons/s cm<sup>2</sup>. This indicates that third order transition probabilities are the same for TPIP and *z*-scan.

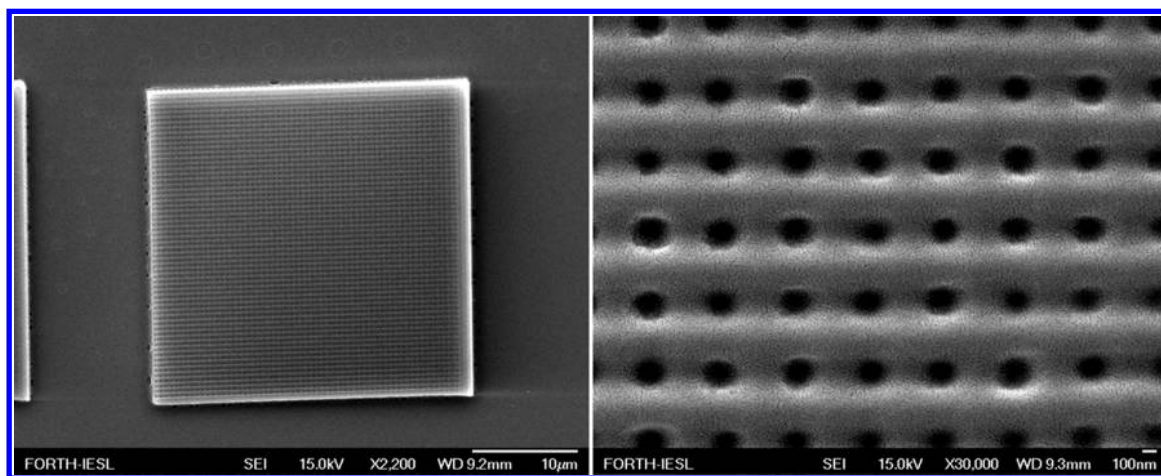


**Figure 3.** Woodpile photonic crystals with 500 nm interlayer periodicity fabricated by TPIP using **3c** as a radical initiator.

## CONCLUSIONS

In conclusion, by using two-step protocol and mild oxidizing agent it is possible to obtain D–A type acyl–phosphine oxides bearing basic nitrogen atoms. Experimental results clearly indicate that the acyl–phosphine oxide chromophores exhibit measurable TPA cross-section only if the strongest electron-donating groups are present. Using such acyl–phosphine oxide possessing push–pull structure as initiator, 3D nanopatterns were successfully fabricated by TPIP. Our results showed that the electron-donating ability as well as the solubility significantly affected the two-photon initiation efficiency. This study constitutes a valuable reference for further research in designing and synthesis of new TPIP initiators.

## ASSOCIATED CONTENT

### Supporting Information

<sup>1</sup>H NMR and <sup>13</sup>C NMR spectra of compounds **2a–2e** and **3a–3e**. This material is available free of charge via the Internet at <http://pubs.acs.org>.

## AUTHOR INFORMATION

### Corresponding Author

\*E-mails: [dtgryko@icho.edu.pl](mailto:dtgryko@icho.edu.pl) and [mfarsari@iesl.forth.gr](mailto:mfarsari@iesl.forth.gr).

### Author Contributions

The manuscript was written through contributions of all authors. All authors have given approval to the final version of the manuscript.

### Notes

The authors declare no competing financial interest.

## ACKNOWLEDGMENTS

The research leading to these results has received funding from the European Community's Seventh Framework Marie Curie ITN program TopBio (PITN-GA-2010-264362).

## REFERENCES

- (1) (a) Juodkazis, S.; Mizeikis, V.; Misawa, H. *J. Appl. Phys.* **2009**, *106*, 051101. (b) Sekkat, Z.; Kawata, S. *Laser & Photon. Rev.* **2012**, DOI: 10.1002/lpor.201200081.
- (2) (a) Radke, A.; Gissibl, T.; Klotzbücher, T.; Braun, P. V.; Giessen, H. *Adv. Mater.* **2011**, *23*, 3018–3021. (b) Vasilantonakis, N.; Terzaki, K.; Sakellari, I.; Purlys, V.; Gray, D.; Soukoulis, C. M.; Vamvakaki, M.; Kafesaki, M.; Farsari, M. *Adv. Mater.* **2012**, *24*, 1101–1105.
- (3) Tian, Y.; Zhang, Y. L.; Ku, J. F.; He, Y.; Xu, B. B.; Chen, Q. D.; Xia, H.; Sun, H. B. *Lab Chip* **2010**, *10*, 2902–2905.
- (4) Gansel, J. K.; Thiel, M.; Rill, M. S.; Decker, M.; Bade, K.; Saile, V.; von Freymann, G.; Linden, S.; Wegener, M. *Science* **2009**, *325*, 1513–1515.
- (5) (a) Torgersen, J.; Ovsianikov, A.; Mironov, V.; Pucher, N.; Qin, X. H.; Li, Z. Q.; Cicha, K.; Machacek, T.; Liska, R.; Jantsch, V.; Stampfl, J. *J. Biomed. Opt.* **2012**, *17*. (b) Raimondi, M. T.; Eaton, S. M.; Laganà, M.; Aprile, V.; Nava, M. M.; Cerullo, G.; Osellame, R. *Acta Biomaterialia* **2013**, *9*, 4579–4584. (c) Melissinaki, V.; Gill, A. A.; Ortega, I.; Vamvakaki, M.; Ranella, A.; Haycock, J. W.; Fotakis, C.; Farsari, M.; Claeysens, F. *Biofabrication* **2011**, *3*, 045005.
- (6) Gu, M. Presented at CLEO/Europe-IQEC, 2013.
- (7) von Freymann, G.; Ledermann, A.; Thiel, M.; Staud, I.; Essig, S.; Busch, K.; Wegener, M. *Adv. Funct. Mater.* **2010**, *20*, 1038–1052.
- (8) Malval, J. P.; Jin, M.; Morlet-Savary, F.; Chaumeil, H.; Defoin, A.; Soppera, O.; Scheul, T.; Bouriau, M.; Baldeck, P. L. *Chem. Mater.* **2011**, *23*, 3411–3420.
- (9) (a) Rajaram, A.; Chen, X.-.; Schreyer, D. *J. Tissue Eng., Part B: Rev.* **2012**, *18*, 454–467. (b) Spangenberg, A.; Malval, J.-P.; Akdas-Kilig, H.; Fillaut, J.-L.; Stehlin, F.; Hobeika, N.; Morlet-Savary, F.; Soppera, O. *Macromolecules* **2012**, *45*, 1262–1269. (c) Baldacchini, T. *Three-Dimensional Microfabrication by Two-Photon Polymerization*. In *Generating Micro- and Nanopatterns on Polymeric Materials*; del Campo, A., Arzt, E., Eds.; Wiley-VCH: Weinheim, Germany, 2011; pp 107–140. (d) Belfield, K. D.; Ren, X. B.; Van Stryland, E. W.; Hagan, D. J.; Dubikovskiy, V.; Miesak, E. J. *J. Am. Chem. Soc.* **2000**, *122*, 1217–1218. (e) Belfield, K. D.; Schafer, K. J.; Liu, Y. U.; Liu, J.; Ren, X. B.; Van Stryland, E. W. *J. Phys. Org. Chem.* **2000**, *13*, 837–849. (f) Gill, A. A.; Claeysens, F. *Two-Photon Polymerization for Tissue-Engineered Scaffold Fabrication*. In *Optical Techniques in Regenerative Medicine*; Morgan, S. P., Rose, F. R., Matcher, S. J., Eds.; Taylor & Francis: Abingdon, U.K., 2013; pp 93–114.
- (10) (a) Schafer, K. J.; Hales, J. M.; Balu, M.; Belfield, K. D.; Van Stryland, E. W.; Hagan, D. J. *J. Photochem. Photobiol., A: Chem.* **2004**, *162*, 497–502. (b) Xue, J.; Zhao, Y.; Wu, J.; Wu, F. *J. Photochem. Photobiol., A* **2008**, *195*, 261–266. (c) Li, Z.; Pucher, N.; Cicha, K.; Torgersen, J.; Ligon, S. C.; Ajami, A.; Husinsky, W.; Rosspeintner, A.; Vauthey, E.; Naumov, S.; Scherzer, T.; Stampfl, J.; Liska, R. *Macromolecules* **2013**, *46*, 352–361.
- (11) Reinhardt, B. A.; Brott, L. L.; Clarson, S. J.; Dillard, A. G.; Bhatt, J. C.; Kannan, R.; Yuan, L. X.; He, G. S.; Prasad, P. N. *Chem. Mater.* **1998**, *10*, 1863–1874.
- (12) Shioji, K.; Matsumoto, A.; Takao, M.; Kurauchi, Y.; Shigetomi, T.; Yokomori, Y.; Okuma, K. *Bull. Chem. Soc. Jpn.* **2007**, *80*, 743–746.
- (13) Zheng, Q. D.; He, G. S.; Prasad, P. N. *J. Mater. Chem.* **2005**, *15*, 579–587.
- (14) Brar, A. S.; Gandhi, S.; Markanday, M. *J. Mol. Struct.* **2005**, *734*, 35–44.

- (15) Keglevich, G.; Toth, V. R.; Drahos, L. *Heteroatom Chem.* **2011**, *22*, 15–17.
- (16) Lindner, E.; Huebner, D. *Chem. Ber.* **1983**, *116*, 2574–2590.
- (17) (a) Macarie, L.; Petrean, A.; Ilia, G.; Iliescu, S.; Popa, A.; Abadie, M. J. M. *J. Polym. Res.* **2005**, *12*, 331–337. (b) Bhuian, B.; Winfield, R. J.; O'Brien, S.; Crean, G. M. *Appl. Surf. Sci.* **2005**, *252*, 4845–4849.
- (18) Sheik-Bahae, M.; Said, A. A.; Wei, T. H.; Hagan, D. J.; Van Stryland, E. W. *IEEE J. Quantum Electron.* **1990**, *26*, 760–769.
- (19) (a) Sakellari, I.; Gaidukeviciute, A.; Giakoumaki, A.; Gray, D.; Fotakis, C.; Farsari, M.; Vamvakaki, M.; Reinhardt, C.; Ovsianikov, A.; Chichkov, B. N. *Appl. Phys. A: Mater. Sci. Process.* **2010**, *100*, 359–364. (b) Sakellari, I.; Kabouraki, E.; Gray, D.; Purlys, V.; Fotakis, C.; Pikulin, A.; Bityurin, N.; Vamvakaki, M.; Farsari, M. *ACS Nano* **2012**, *6*, 2302–2311.
- (20) Ovsianikov, A.; Viertel, J.; Chichkov, B.; Oubaha, M.; MacCraith, B.; Sakellari, L.; Giakoumaki, A.; Gray, D.; Vamvakaki, M.; Farsari, M.; Fotakis, C. *ACS Nano* **2008**, *2*, 2257–2262.
- (21) (a) Miyazaki, K.; Horibe, T. *J. Biomed. Mater. Res.* **1988**, *22*, 1011–1022. (b) Bland, M. H.; Peppas, N. A. *Biomaterials* **1996**, *17*, 1109–1114. (c) Park, Y. J.; Chae, K. H.; Rawls, H. R. *Dent. Mater.* **1999**, *15*, 120–127. (d) Jandt, K. D.; Mills, R. W.; Blackwell, G. B.; Ashworth, S. H. *Dent. Mater.* **2000**, *16*, 41–47.
- (22) Miller, R. C.; Miller, C. D.; Rogers, W.; Hamilton, L. A. *J. Am. Chem. Soc.* **1957**, *79*, 424–427.
- (23) Fischer, M. et al. U. S. Patent 5,679,863, Oct. 11, 1997.
- (24) Su, W. C. et al., U. S. Patent 7,465,819, B2, Dec. 16, 2008.
- (25) Wan, Y. L.; Ping, H.; Yu, X. G.; Peng, L.; Yu, F. Z. *Acta Crystallogr.* **2007**, *E63*, 1008–1009.
- (26) Ho, K. M.; Chan, C. T.; Soukoulis, C. M.; Biswas, R.; Sigalas, M. *Solid State Commun.* **1994**, *89*, 413–416.
- (27) Fischer, J.; Wegener, M. *Opt. Mater. Express* **2011**, *1*, 614–624.